RR-43

ISSN 0252-1075
Research Report No. RR-043

CONTRIBUTIONS FROM

INDIAN INSTITUTE OF TROPICAL METEOROLOGY

THE NUMERICAL EXPERIMENTS WITH INCLUSION OF OROGRAPHY IN FIVE LEVEL P. E. MODEL IN PRESSURE-COORDINATES FOR INTERHEMISPHERIC REGION

BY

S. N. BAVADEKAR

AND

R. M. KHALADKAR

PUNE - 411 005

INDIA

MARCH 1989

R. M. Khaladkar

The numerical experiments with inclusion of orography in five level P.E. model in pressure-coordinates for interhemispheric region.

RR-43

S.N. Bavadekar and R.M. Khaladkar

Indian Institute of Tropical Meteorology, Pune-411005.

ABSTRACT

A regional five level P.E. model in x, y, p, t coordinate system is tested for simulation of the orographic effect on atmospheric motion for interhemispheric region. The model domain extends from 24°E to 102°E and 28°S to 40°N.

The initial values for the five-level P.E. model are prepared from the observed zonal wind profile having meridional and vertical wind shears typical of July, for the section of the longitude 62.5°E. The sea level pressure values, for this section, are also obtained. The initial data prepared for this section are assumed to represent for the whole domain of the model. The orography in the domain from 16°S to 28°N and 36°E to 90°E is included in the model. The domain thus includes the orography of east African continent, south part of Saudi Arabia, Pakistan, India etc.

The model is integrated for 48-hours with the initial data and the forcing due to orography as mentioned above. The results of integration show that the orography of east African continent is important for the development of low level cross-equatorial flow and the strong winds off Somali. The orography of peninsular India also plays some role in low level development of circulation over Indian region. The simulated flow fields are presented in the paper and the results are discussed.

1. Introduction

A regional five-level P.E. model in pressure co-ordinates is being tested in the Indian Institute of Tropical Meteorology, Pune. The simplified version of this model was used by Singh and Saha (1976) for the case of monsoon depression at the head Bay of Bengal. The purpose of their experiment was to test the computational stability of the finite-difference schemes. Subsequently the model is developed further to include various physical processes such as transfer of momentum, heat and moisture in boundary layer, latent heat release due to large-scale condensation and convective heat and moisture transports etc. (Singh,

1985, Singh et al. 1988). The model, however, did not include the mountains and their effects on atmospheric flows.

The orography, on all scales, influences atmospheric motions. The atmospheric flow is deflected horizontally and vertically and retarded at the surface due to orography. The orography also provides the elevated sources of sensible and latent heat. The inclusions of mountains in the numerical experiments conducted by Hahn and Manabe (1975), Kasahara (1973), Manabe and Terpstra (1974) etc. have brought out the importnce of the orography on improved simulation of the atmospheric flows. The numerical treatment in presence of orography is, however, required to be applied with proper care. It should ensure that the numerical results of various physical processes included in the model are contaminated as little as possible by the effects that may be caused by its application.

The computational design of the limited area multilevel P.E. model in pressure coordinates with inclusion of orography is given by Okamura (1975). Bavadekar and Khaladkar (1986a) developed the computer program for 3 level P.E. model and tested it successfully for the simple

experiment of uniform westerly flow crossing the large elliptic barrier with maximum height of one km. The computational procedure for three level P.E. model with inclusion of orography is given by Okamura (1976). Bavadekar and Khaladkar (1986b) also tested the model for the orography of peninsular India and neighbouring regions for the typical zonal wind flow over India during summer monsoon. The trough in the head Bay of Bengal is formed in the lower troposphere as a result of interaction. The results of of simulation are in agreement with the findings of Banerjee (1930), Gadgil (1977) and Gadgil and Sikka (1976). Das and Bedi (1976, 1978) also have performed the experiments with three level P.E. model in σ coordinates. In addition to the orography of peninsular India, the elliptic orography resembling the size of Himalaya is also included in the model. The lee trough due to orography of peninsular India is not apparent in their results. The monsoon trough, however, is well simulated when thermal forcing is considered (Das and Bedi 1979, 1981).

2. Brief description of the model

The computational design for multilevel P.E. model in pressure coordinates is given by Okamura (1975).

The five-level version of the P.E. model based on this design is adopted for the present study. As our main interest is to simulate the dynamic effects of orography on the large-scale motion, the model atmosphere is assumed to be dry in the present study. The equation for water vapour and the associated physical processes are, therefore, not considered in this investigation. The governing equations of P.E. model are given as

$$\frac{\partial u}{\partial t} + m^2\left\{\frac{\partial}{\partial x}\left(u\frac{u}{m}\right)+\frac{\partial}{\partial y}\left(u\frac{v}{m}\right)\right\}+\frac{\partial}{\partial p}(u\omega)$$

$$-f^*v + m\frac{\partial \phi}{\partial x} = F_x \qquad (2.1)$$

$$\frac{\partial v}{\partial t} + m^2\left\{\frac{\partial}{\partial x}\left(v\frac{u}{m}\right)+\frac{\partial}{\partial y}\left(v\frac{v}{m}\right)\right\}+\frac{\partial}{\partial p}(v\omega)$$

$$+f^*u + m\frac{\partial \phi}{\partial y} = F_y \qquad (2.2)$$

$$\frac{\partial \phi}{\partial p} = -\frac{RT}{p} \qquad (2.3)$$

$$m^2\left\{\frac{\partial}{\partial x}\left(\frac{u}{m}\right)+\frac{\partial}{\partial y}\left(\frac{v}{m}\right)\right\}+\frac{\partial \omega}{\partial p} = 0 \qquad (2.4)$$

$$\frac{\partial}{\partial t}(C_p T) + m^2\left\{\frac{\partial}{\partial x}\left(C_p T \frac{u}{m}\right) + \frac{\partial}{\partial y}\left(C_p T \frac{v}{m}\right)\right\}$$

$$\frac{\partial}{\partial p}(C_p T\omega) + \frac{\partial \phi}{\partial p}\omega = D_t \qquad (2.5)$$

where u, v, ω, ϕ, T are the dependent variables. u and v are the wind components in X and Y directions, ω, the vertical p-velocity, ϕ, the geopotential and T, the temperature. R, C_p and m are the gas constant for dry air, specific heat at constant pressure and the map factor respectively.

f* is given by

$$f^* = f + m^2\left\{v\frac{\partial}{\partial x}\left(\frac{1}{m}\right) - u\frac{\partial}{\partial y}\left(\frac{1}{m}\right)\right\} \qquad (2.6)$$

in which f denotes the coriolis parameter, F_x, F_y and D_t are the frictional and diffusion terms.

$$F_x = -k_s u + \nu m^2 \nabla^2 u$$

$$F_y = -k_s v + \nu m^2 \nabla^2 v$$

$$D_t = C_p \nu m^2 \nabla^2 T \qquad (2.7)$$

where $k_s = 5.0 \times 10^{-6}$ sec^{-1} is the coefficient of surface friction and ν is the diffusion coefficient as given by leith (1969)

$$\nu = |\nabla \zeta| d^3$$

Here ζ is the relative vorticity and d is the grid length.

The top of the model atmosphere is assumed at 100 mb

$$\omega = 0 \quad \text{at} \quad p = 100 \text{ mb}$$

At the lower boundary, the condition

$$\frac{\partial p_s}{\partial t} + m \left\{ u_s \frac{\partial p_s}{\partial x} + v_s \frac{\partial p_s}{\partial y} \right\} - \omega_s = 0 \qquad (2.8)$$

is applied.

The vertical structure of the five-level P.E. model is given by figure 1. For the numerical integration, the primitive equations are required to be transformed

into finite difference form. The primitive equations, in flux form, have space differential terms of the type $\frac{\partial}{\partial x}(AB)$ and $A\frac{\partial B}{\partial x}$ etc; where, A and B are arbitrary variables. The finite difference forms of these terms are derived by Okamura (1975) based on the conservation of energy and mass of the system. The finite difference representations of the above two terms are given by

$$D_x(A*B) = \frac{1}{8d\delta_i}\Big[\Big\{A_{i+1}(\delta_{i+1}+\delta_i) + A_i(3\delta_i-\delta_{i+1})\Big\}(B_{i+1}+B_i) - \Big\{A_{i-1}(\delta_{i-1}+\delta_i) + A_i(3\delta_i-\delta_{i-1})\Big\}(B_i+B_{i-1})\Big] \tag{2.9}$$

and

$$G_x(A,B)_i = \frac{1}{4d}\Big\{(A_{i+1}+A_i)(B_{i+1}-B_i) + (A_i+A_{i-1})(B_i-B_{i-1})\Big\} \tag{2.10}$$

respectively.

Here i represent the i^{th} grid point, d the grid length, δ the pressure interval of the layer. Similar notations can be used for the space differential terms in Y - direction.

2.1 Finite difference equations

Using the above notations, the finite difference form of the Primitive equations for 5-level P.E. model can be written as

Equations of motion

$$\frac{\partial u_l}{\partial t} + m^2\left\{D_x\left(u_l * \frac{u_l}{m}\right) + D_y\left(u_l * \frac{v_l}{m}\right)\right\} + \frac{(u_{l+1} + u_l)\omega_l - (u_l + u_{l-1})\omega_{l-1}}{2\delta_l} - f_l^* v_l + \frac{m}{\delta_l} G_x(\delta_l, \phi_l) = F_{x_l} \tag{2.11}$$

$$\frac{\partial v_l}{\partial t} + m^2\left\{D_x\left(v_l * \frac{u_l}{m}\right) + D_y\left(v_l * \frac{v_l}{m}\right)\right\} + \frac{(v_{l+1} + v_l)\omega_l - (v_l + v_{l-1})\omega_{l-1}}{2\delta_l} + f_l^* u_l + \frac{m}{\delta_l} G_y(\delta_l, \phi_l) = F_{y_l} \tag{2.12}$$

where l takes 1, 2, 3, 4 and 5 and

$$\omega_0 = 0 \quad , \quad u_6 = u_5$$

and

$$v_6 = v_5$$

δ_l is the depth of the l^{th} layer.

Hydrostatic equation

$$\frac{\phi_{l+1} - \phi_l}{P_{l+1} - P_l} = - \frac{RT_l}{P_l'} \qquad (2.13)$$

where l = 1,2,3,4 and 5, and

$$\phi_6 = gH$$

g is the acceleration due to gravity and H is the height of orography

$$P_5' = \frac{P_s + P_5}{2}$$

and

$$T_5 = T_4 + \frac{T_4 - T_3}{\delta_4' + \delta_3''} \left(P_5' - P_4' \right)$$

Continuity equation

$$m^2\left\{D_x\left(1*\frac{u_l}{m}\right)+D_y\left(1*\frac{v_l}{m}\right)\right\}+\frac{\omega_l-\omega_{l-1}}{\delta_l}=0 \qquad (2.14)$$

where l = 1, 2, 3, 4, and 5.

and

$$\omega_5=\omega_s$$

Thermal equation

$$\frac{\partial}{\partial t}(C_pT_l)+\frac{m^2}{\delta_l'+\delta_l''}\left[\left\{D_x'\left(C_pT_l*\frac{u_l}{m}\right)+D_y'\left(C_pT_l*\frac{v_l}{m}\right)\right\}\delta_l'\right.$$

$$\left.+\left\{D_x''\left(C_pT_l*\frac{u_{l+1}}{m}\right)+D_y''\left(C_pT_l*\frac{v_{l+1}}{m}\right)\right\}\delta_l''\right]$$

$$+C_p\frac{F_{l+1}-F_l}{4(\delta_l'+\delta_l'')}+\frac{\phi_{l+1}-\phi_l}{\delta_l'+\delta_l''}\omega_l=D_{t_l} \qquad (2.15)$$

where l = 1, 2, 3, 4

$$F_1 = 0$$

$$F_l = (T_l + T_{l-1})(\omega_l + \omega_{l-1}),$$

$$l = 2, 3, 4$$

$$F_5 = 4 T_l \omega_s$$

Here D_x' and D_x'' indicate that they must be applied to the layers δ_l' and δ_l'' respectively.

Tendency equation

$$\frac{\partial P_s}{\partial t} + m^2 \left\{ G_x\left(\frac{u_5}{m}, P_s\right) + G_y\left(\frac{v_5}{m}, P_s\right) \right\} - \omega_s = 0 \qquad (2.16)$$

The above difference equations can be solved for model domain. The cyclic boundary conditions are assumed for the east and west and for north and south, rigid walls are assumed with no flow across these walls.

2.2 Special difference equations

At the points near the orography the special finite difference schemes as given by Okamura (1975) are used. For example at (i + 1)th point, in Fig. 1 , P_s becomes less than P_c where

$$P_c = \frac{P_2' + P_3}{2} = 550 \text{ mb}$$

The difference scheme at i^{th} and $(i+1)^{th}$ points are

$$D_x\left(A * \frac{u_3}{m}\right)_i = -\frac{1}{8d\delta_{3,i}}\left[\left\{A_{i-1}\left(\delta_{3,i-1} + \delta_{3,i}\right) + A_i\left(3\delta_{3,i} - \delta_{3,i-1}\right)\right\}\right]\left\{\left(\frac{u_3}{m}\right)_i + \left(\frac{u_3}{m}\right)_{i-1}\right\} \tag{2.17}$$

and

$$D_x\left(A * \frac{u_2}{m}\right)_{i+1} = \frac{1}{8d\delta_{2,i+1}}\left[\left\{A_{i+2}\left(\delta_{2,i+2} + \delta_{2,i+1}\right) + A_{i+1}\left(3\delta_{2,i+1} - \delta_{2,i+2}\right)\right\}\left\{\left(\frac{u_2}{m}\right)_{i+2} + \left(\frac{u_2}{m}\right)_{i+1}\right\} - 2\delta_{2,i}\left(A_i + A_{i+1}\right)\left\{\left(\frac{u_2}{m}\right)_{i+1} + \left(\frac{u_2}{m}\right)_i\right\}\right] \tag{2.18}$$

where A takes the values of u, v or 1.

$$G_x(\delta_3, \phi_3)_i = \frac{1}{2d}(\delta_{3,i} + \delta_{3,i-1})(\phi_{3,i} - \phi_{3,i-1})$$

and,

$$G_x(\delta_2, \phi_2)_{i+1} = \frac{1}{4d}(\delta_{2,i+2} + \delta_{2,i+1})(\phi_{2,i+2} - \phi_{2,i+1})$$

$$+ 2\delta_{2,i}(\phi_{2,i+1} - \phi_{2,i})\}$$

For tendency equation the schemes

$$G_x(u_3, P_s)_i = \frac{1}{4d}(u_{3,i} + u_{3,i-1})(P_{s_i} - P_{s_{i-1}})$$

and

$$G_x(u_2, P_s)_{i+1} = \frac{1}{4d}(u_{2,i+2} + u_{2,i+1})(P_{s_{i+2}} - P_{s_{i+1}})$$

are used.

At the white marked points, the predicted temperatures should be given by the application of horizontal mean,

$$T_{i,j} = (T_{i+1,j} + T_{i-1,j} + T_{i,j+1} + T_{i,j-1}) / 4.0$$

instead of using the thermal equation 2.15. The averaging is applied only after the temperatures at the white points are obtained by interpolation.

At the cross point which is under orography no computation is required.

3. Orography

The horizontal domain of the model is shown in Fig. 2. The model domain extends from 24°E to 102°E and 28°S to 40°N, with latitude/longitude grid of 2°. Inside the model domain orography is shown. it extends from 36°E to 90°E and 16°S to 28°N.

The values of orographic heights are taken from the tabulation of Gates and Nelson (1975). The orography of east African continent, part of Saudi Arabia, Pakistan, India etc. comes under this region.

No smoothing is applied for the observed orographic heights but, as is apparent, the orographic heights at some locations are not actual. For example, the orographic heights at the grid points in the Gulf of Aden, Red sea etc. are not zero. These are the narrow channels and

the grid points at lower levels are situated in the valley of mountains. The height at such grid point is changed in such a way that it is not locked in the valley of mountains in both x and y directions. This is done because the finite difference schemes can not be applied for such points.

The care is also necessary for the point for which the computed surface pressure value at the initial time is close to either of the pressure levels 600, 800 and 950 mb and the pressure difference is less than about 10 mb. The computed pressure difference at such point is set to 10 mb at the beginning by changing the height of the orography. This procedure ensures that the points under orography are not changing their locations due to rapid changes in surface pressure values and not coming out as data void points at least at the early period of forecasts. The modified orographic heights are shown in inner domain of the fig. 2.

4. Initial values

The initial values are obtained from the observed circulation over Arabian sea during July. The observed

flow during northern summer shows very strong winds off Somali coast in Indian ocean. The high winds are part of the much larger circulation which has its origin in the southern hemisphere. The flow usually crosses the equator in a fairly narrow band of width 500 km near Kenya coast and is confined to lowest 2 to 3 km. The flow is also controlled to a large extent by the monsoon trough over India with associated low level convergence. In the southern hemisphere the low level divergence is associated with the subtropical high pressure belt.

At the west coast of India the low level westerly flow crosses the barrier of Western Ghats and generates the northerly component of the wind just on the lee side. The low level flow turns cyclonically on the lee side with the trough in the head Bay of Bengal. The axis of the summer monsoon trough at the surface runs from Ganganagar to Calcutta through Allahabad. The trough line is seen in the upper air also up to about 6 km. The trough line is sloping southwards with height and at 600 mb it runs from Bombay to Sambalpur.

Fig. 3 shows the initial zonal wind profile having meridional and vertical wind shears, typical of July,

for the longitude section of 62.5°E. The initial sea level pressure for July for this section is also shown in fig.4. From the zonal wind the geopotential height is obtained by using geostrophic approximation. The temperatures at different levels are obtained by using the equation 2.13 and assuming no mountains. The initial values, thus prepared, for longitude section of 62.5°E, are assumed to represent for whole domain of the model. The orography as shown in fig. 2 is now included and the surface pressure values are computed using the equation 2.13 again.

Since the purpose of present study is to test the model performance for interhemispheric region with forcing due to orography, we have used the simplified initial values as input to the model.

5. Simulation experiments

Using the orography and the initial values as prepared above, the experiments are performed by integrating the model for 48-hours each. Matsuno's (1966) time-integration scheme is used for the marching process with the time-step of 5 minutes. The provision is made, in

computer program, to compute the values of

$$\sum_{1}^{N} |u^{\tau+\Delta\tau} - u^{\tau}|$$

and,

$$\sum_{1}^{N} |v^{\tau+\tau\Delta} - v^{\tau}|$$

for every time-step. Here τ represents the time and $\Delta\tau$ the time-step. The quantities under summation signs represent the absolute values of the predicted changes in wind components at every time step at particular grid point. The summation extends over all the grid points for all the levels of the model. These values are plotted in fig.5. After 24 hours the values become very small and more or less steady. The model can be integrated beyond 48-hours but without any further improvement in results. The forecast fields for 48-hours are, therefore, presented in the paper. The experiments as mentioned below are conducted.

(1) The experiment one is performed by using the complete orography of the inner domain of fig.2. This experiment is referred to as 'All orography' or AO-experiment.

(ii) The experiment two is performed without the orography of India. The orography east of 66°E is set to zero in the initial data. This experiment is referred to as, 'without India' or WI-experiment.

(iii) The experiment three is performed without the orography of East-African continent, Saudi Arabia etc. The orography west of 66°E is set to zero in the initial data for this case. This experiment is referred to as 'without Africa' or WA-experiment.

The WI and WA experiments are performed to assess the effect of removal of orography of India and Africa respectively on the low level evolution of the flow. The results of these experiments are presented below.

5.1 Results of simulation experiments

Winds : The figures 6 through 10 show the forecast winds for 200, 400, 600, 800 and 950 mb levels respectively for the experiment - AO. The winds at the inner domain only are shown. The winds at 200 mb and 400 mb are not affected much due to orography. The winds at 600 mb level

are anticyclonic over Indian ocean with the centre situated at 55°E over the equator. West of 55°E the cross-equatorial flow is southerly. Over the east coast of India, cyclonic circulation is developed for this level. The centre of the cyclonic circulation is situated at about 15°N, 84°E.

At 800 mb level the anticyclonic circulation is somewhat stronger over Indian ocean. The centre of the anticyclonic circulation is situated on equator at about 63°E. The cross-equatorial flow off Kenya coast and the strong winds off Somali coast are also seen. The flow over India is cyclonic with the centre approximately at 23°N, 83°E. At the lowest level (950 mb) the features of cross equatorial flow and the strong winds of about 40 knots off Somali-coast are seen. The winds over India are cyclonic and the axis of the cyclonic circulation is along 27°N. From the results it is apparent that the cyclonic circulation developed over India has southward tilt in the vertical.

WI-experiment is performed to assess the effect of removal of Indian orography in the initial data on the circulation over this region. The forecast winds for 600, 800 and 950 mb are shown in figures 11,12 and 13 respectively. The simulated flow over Indian ocean

and Arabian sea is not affected due to removal of Indian orography but the circulation over Indian region is certainly affected. All the previous features of cyclonic circulation of AO-experiment are not developed over this region.

In WA-experiment the African orography is removed from the initial data. The forecast winds for 600, 800 and 950 mb levels are shown in figures 14, 15 and 16 respectively. The results show that circulation features over Indian region similar to AO-experiment, are established but the circulation over Indian ocean and Arabian sea is radically changed. There is no close anticyclonic circulation over Indian ocean. The cross-equatorial flow at 600 mb and 800 mb levels off Kenya coast is in opposite direction, i.e. northerly wind is developed instead of southerly. At 950 mb, however, uniform southerly wind component is developed along the equator but the strong winds off Somali are not developed.

The results of these experiments show that the low level evolution of the flow is directly affected by the orography. The importance of Indian orography, although of low height, on development of low level cyclonic circulation has been brought out in this study. The orography

of east African continent also plays a dominant role for development of cross-equatorial flow and strong winds off Somali.

Surface pressure change : In fig. 17 the surface pressure change for AO-and WI-experiments is compared. The high pressure developed on the northern periphery of Saudi-Arabia is found to be elongated eastward. Low pressure is developed in the southern part of the domain. The pressure change is about-4 mb over southern part of Saudi Arabia and northern tip of Somali.

The low pressure observed over India in AO-experiment is absent in WI-experiment. These results show that the inclusion of orography alone is unable to produce the summer monsoon trough over India. The effect of thermal forcing is not included in the present investigation but the factor is important for the proper development of monsoon trough.

Temperature change and the vertical p-velocity : In figure 18 the temperature changes at 300 mb level are compared for AO-and WI-experiments. In general, cooling is observed on the northern side of the orographic domain and warming on the southern side. In AO-experiment warming

is found over northern side of India which is shifted further northward for WI-experiment. Cooling and warming, in general, are produced due to forced ascent and descent respectively of the flow due to orography. The temperature is also changed due to advection of the winds.

The vertical p-velocity for AO-and WI-experiments is compared in figure 19. The vertical p-velocity is upward in the northern part of orographic domain and downward in the southern part.

The temperature changes and vertical p-velocity show similar features for 500-mb but for the want of space these figures are not shown.

The temperature changes at 700 and 900 mb also show more or less similar features with cooling in the northern side of the orographic region and warming on the southern side. At these levels the temperature at white points in the orographic regions are computed by averaging after interpolation from the neighbouring points. For the want of space the temperature changes for 700 and 900 mb are not shown.

The vertical p-velocity for 700 mb for AO-and WI-experiments are compared in fig. 20. The vertical velocity is having complicated features over Saudi Arabia and Somali regions. Over the central India the vertical velocity is upward and at the east-coast it is downward for AO-experiment.

Over India the vertical velocity is upward throughout in WI-experiment. The effect of peninsular India orography, thus appears to be important for downward velocity at the east coast.

The vertical velocity pattern is very much complicated in the orographic region for 900 mb level. The vertical velocity for 900 mb is not shown.

Vorticity field : The relative and absolute vorticity fields are computed for different levels for WI-experiment. The absolute vorticity is positive to the north of the equator and negative to the south of the equator. The absolute vorticity for 950 mb is shown in figure 21. The relative vorticity for 800 and 950 mb is shown in figure 22. The axis of the strong winds off Somali is found to be coincident with zeroth isopleth of relative vorticity at these levels.

Cross-equatorial flow : Fig. 23 shows the meridional wind across the equator for AO-experiment. Southerly wind core of 8.3 mps is found at 950 mb level at 52°E. The cross-equatorial flow on the eastern part above 950 mb is northerly. Anderson (1980) has given delightful survey on the orographically controlled cross-equatorial flows. The simulation of Findlater jet is attempted analytically and numerically by different workers. The observed core of the cross-equatorial flow for July is situated at 900 mb at about 40°E and the speed is about 30 knots (Findlater 1969). The observed flow, however, can not be compared with the model results as the winds at 900 mb are not available and also the forcing due to other factors apart from orography are not considered in this simple experiment.

6. Concluding remarks

The five level P.E. model in pressure coordinates is successfully integrated for inter-hemispheric region with the initial data as mentioned in the text. The forcing due to orography as shown in fig. 2, is included in the

model integration. The computer program was run on NEC-S 1000 computer, Pune. The results show that the orography of east African continent is important for development of cross-equatorial flow and strong winds off Somali coast. The orography of India is also important for the low level evolution of the flow over Indian region. These results show that the model performance is satisfactory in simulating the dynamic effects of orography on the large-scale atmospheric flows.

The domain of orography considered in the present investigation did not include the high mountains of Tibet. The thermal forcing effect is also not considered in the present study. The experiments with inclusion of these effects will be conducted subsequently.

Acknowledgement

The authors' grateful thanks are due to Director, Shri D.R. Sikka, for stimulating discussion and encouragement throughout the work. Thanks are due to Dr. S.S. Singh, A.D., for critically reviewing the paper and pointing out some of the obvious mistakes in the write-up. Thanks are also due to drawing and photo units of the Institute for preparing the diagrams and to Smt. C. Bardhan for typing the manuscript.

References

Anderson, D.L.T., 1980 : Orographically controlled cross-equatorial flow, GARP Publication series No. 23, Orographic effects in planetary flows, Chapter 10, pp. 317-355.

Banerjee, S.K., 1930 : The effect of Indian mountain ranges on the configuration of isobars, Indian Journal of Physics, 4, 477-502.

Bavadekar, S.N. and Khaladkar, R.M., 1986a : Dynamic effects of orography on the large-scale motion of the atmosphere-zonal flow and elliptic barrier with maximum height of one km., Mausam, 37, 1, 55-60.

Bavadekar, S.N. and Khaladkar, R.M., 1986b : Some aspects of large scale lee-waves due to westerly flow over peninsular India; Mausam, 37, 4, 483-490.

Das, P.K. and Bedi, H.S., 1976 : A study on orographic effects by a primitive equation model, Proc. Symp. on Tropical Monsoons, IITM, 51-58.

Das, P.K. and Bedi, H.S., 1978 : The inclusions of Himalayas in Primitive equation model, Indian J. Met. Hydrol. Geophys., 375-383.

Das, P.K. and Bedi, H.S., 1979 : Numerical simulation of monsoon circulations; Proc. Indian Acad. Sci., 2, 17-27.

Das, P.K. and Bedi, H.S., 1981 : A numerical model of the monsoon trough, Monsoon Dynamics, Ed. by J. Lighthill and R.P. Pearce. ch. 23, 351-363.

Findlater, J. 1969 : Interhemispheric transport of air in the lower troposphere over the western Indian ocean., Q.J.R. Meteorol. Soc. 95, 400-403.

Gadgil, S. 1977 : Orographic effects of the southwest monsoon., a review. Pure Appl. Geophys. 115, 1413-1430.

Gadgil, S. and Sikka, D.R., 1976 : The influence of the topography of the Indian peninsula on the low level circulation of the summer monsoon. Indian Inst. Sci. Bangalore, Rep. 76, FM-16.

Gates, W.L., and Nelson, A.B. 1975 : A new (revised) tabulation of the Scripps topography on a 1° global grid. Part I : Terrain heights. Rand Corp., R-1276-1-ARPA.

Hahn, D.G. and Manabe, S., 1975 : The role of mountains in the south Asian monsoon circulation., J.Atmos.Sci. 32, 1515-1541.

Kasahara, A., Sasamori, T. Washington, W.M. (1973) : Simulation experiments with a 12-year stratospheric global circulation model, I. Dynamical effect of the Earth's orography and thermal influence of continentality., J. Atmos. Sci., 30, 1229-1251.

Leith, C.E. 1969 : Two dimensional eddy viscosity coefficients, Proc. WMO/IUGG Symposium on NWP. in Tokyo 1965, 1141-44.

Manabe, S. and Terpetra, T.B., 1974 : The effects of mountains on the general circulation of the atmosphere as identified by numerical experiments., J. Atmos. Sci. 31, 3-42.

Matsuno, T. 1966 : Numerical integration of the Primitive equations by a simulated backwward difference method., J. Met. Soc. Japan, 44, 76-84.

Okamura, Y., 1975 : Computational design of a limited area prediction model., J. Met. Soc., Japan 53, 175-188

Okamura, Y., 1976 : Numerical experiments of orographic effect on the large-scale motion of the atmosphere., Pap. Met. Geophys., 27, 1-20.

Singh, S.S. and Saha, K.R., 1976 : Preliminary results of integration of a five level primitive equation model., Proc. Symp. on Trop. Monsoons, IITM, 43-50.

Singh, S.S., Bandyopadhyay, A. and Vaidya, S.S. 1988 : Impact of convective transfer of heat and moisture on the prediction of monsoon depressions., Mausam, 39, 1, 19-26.

Singh, S.S., 1985 : Short range prediction with a multilevel primitive equation model., Proc. Indian Acad. Sci. (Earth and Planetary Sciences), 94, 159-184.

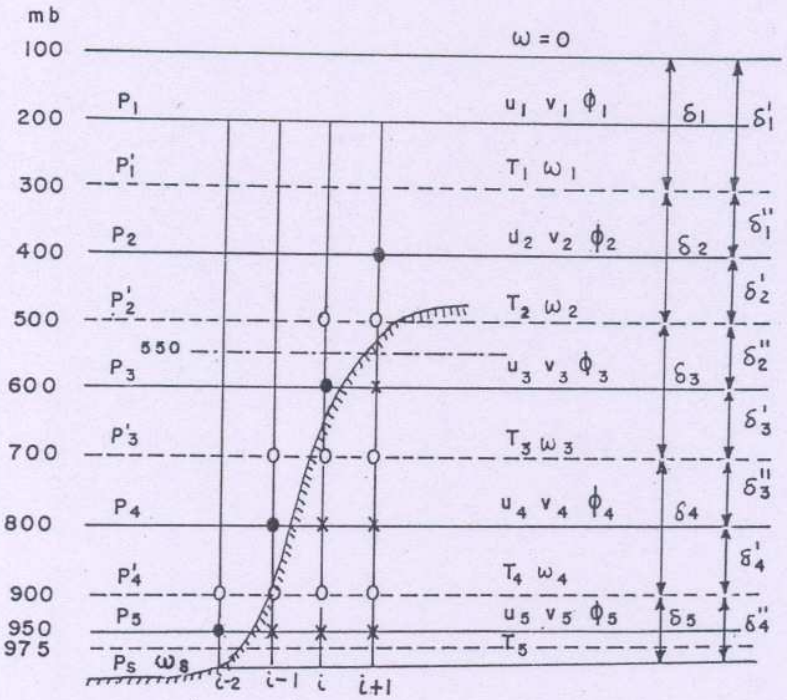

FIG.1 : VERTICAL STRUCTURE OF THE FIVE LEVEL P.E. MODEL

● : BLACK POINT : SPECIAL FINITE DIFFERENCE SCHEMES

X : CROSS POINT : NO COMPUTATIONS

O : WHITE POINT : AVERAGING AFTER INTERPOLATION.

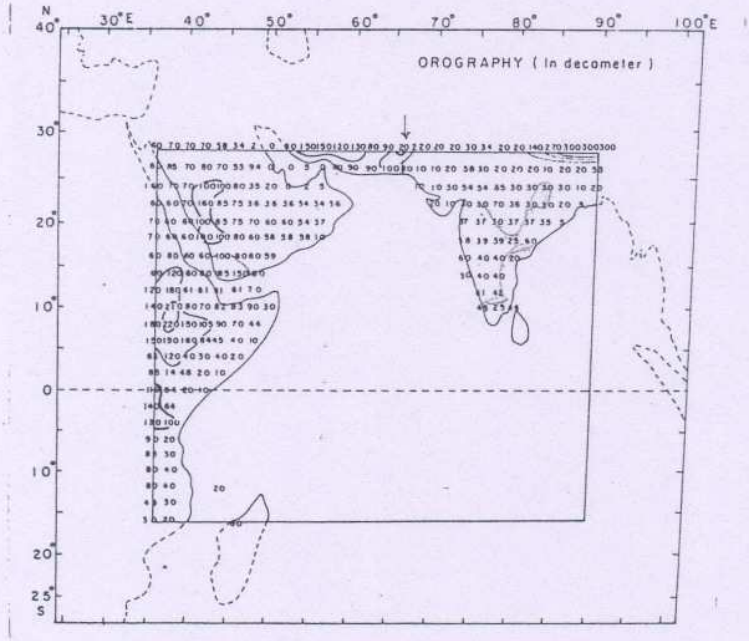

FIG.2 : HORIZONTAL DOMAIN OF THE MODEL

OROGRAPHY IS SHOWN IN THE INNER DOMAIN.

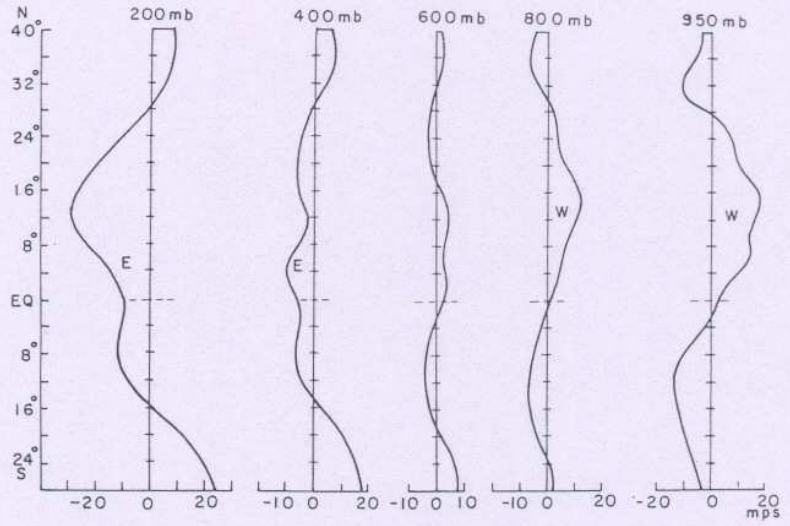

FIG. 3 : INITIAL ZONAL WIND PROFILE AT DIFFERENT LEVELS OF THE MODEL, FOR JULY, FOR THE SECTION OF THE LONGITUDE 62.5°E.

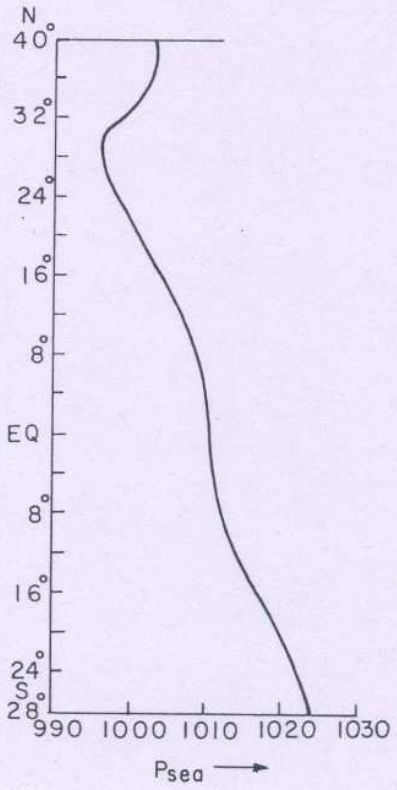

FIG. 4 : INITIAL SEA LEVEL PRESSURE VALUES, FOR JULY, FOR THE SECTION OF THE LONGITUDE 62.5°E.

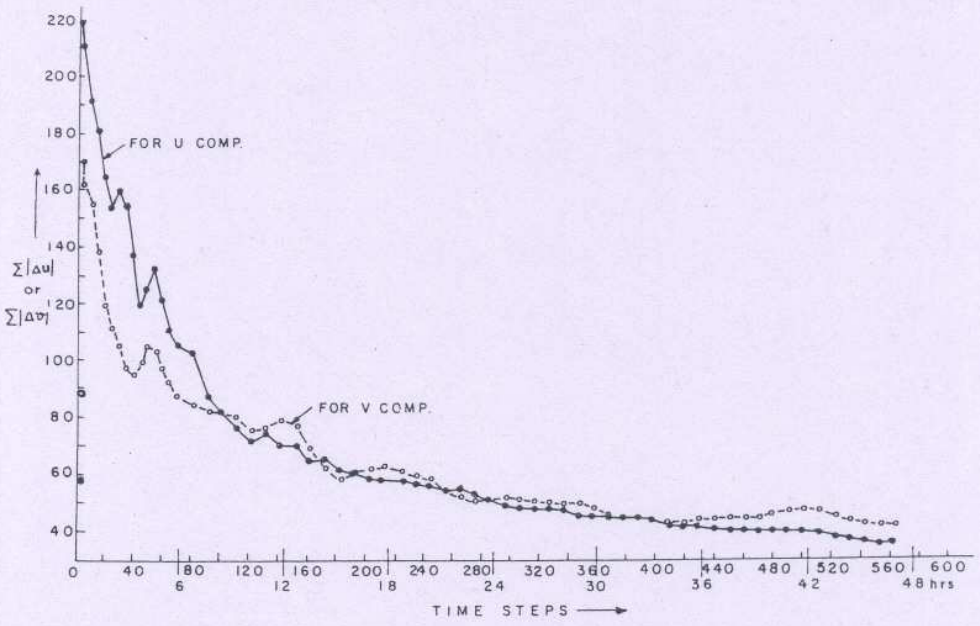

FIG. 5: PLOT OF $\sum_{1}^{N} | u^{\tau+\Delta\tau} - u^{\tau} |$ AND $\sum_{1}^{N} | v^{\tau+\Delta\tau} - v^{\tau} |$ VERSUS TIME-STEPS. THE SUMMATION EXTENDS FOR ALL THE GRID POINTS AT DIFFERENT LEVELS OF THE MODEL. N = 6270.

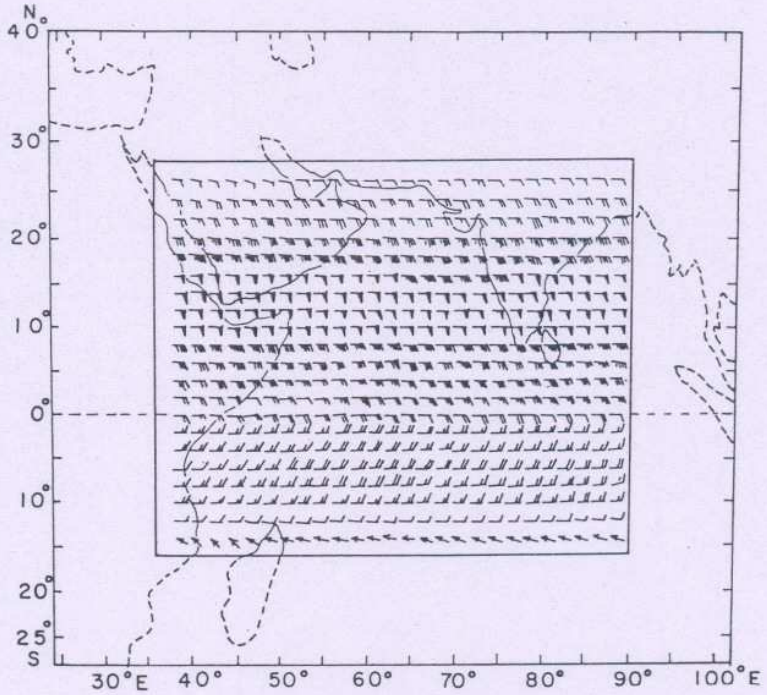

FIG. 6 : FORECAST WINDS AT 200 MB LEVEL FOR AO - EXPT., F.C. : 48 - HOURS.

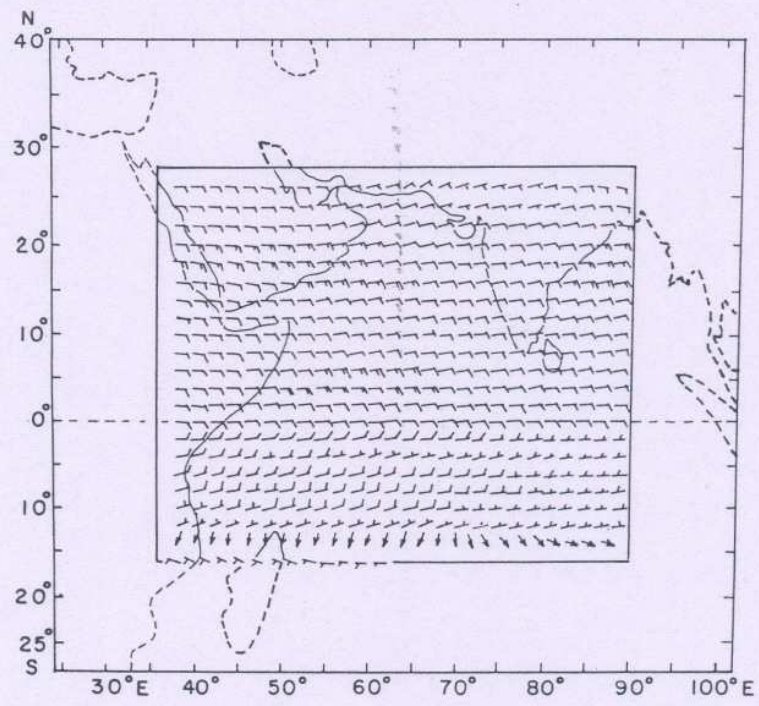

FIG. 7 : FORECAST WINDS AT 400 MB LEVEL AO-EXPT., F.C. : 48-HOURS

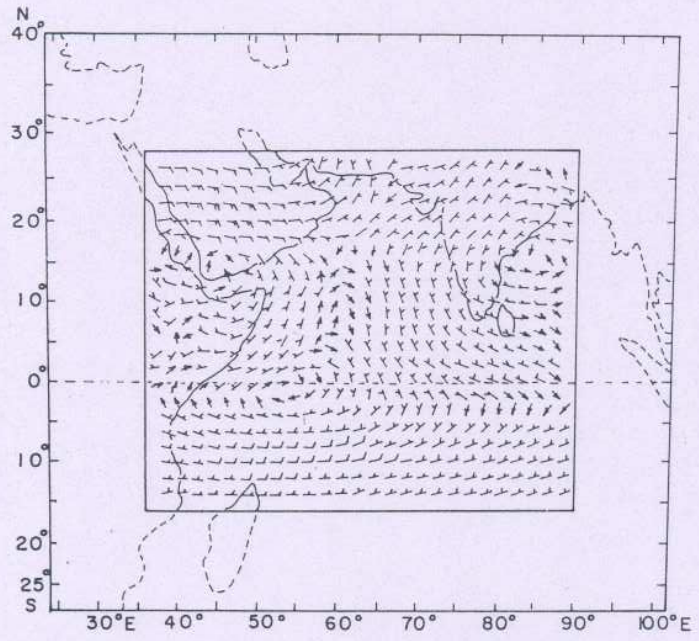

FIG. 8 : FORECAST WINDS AT 600 MB LEVEL

AO-EXPT., F.C. : 48-HOURS

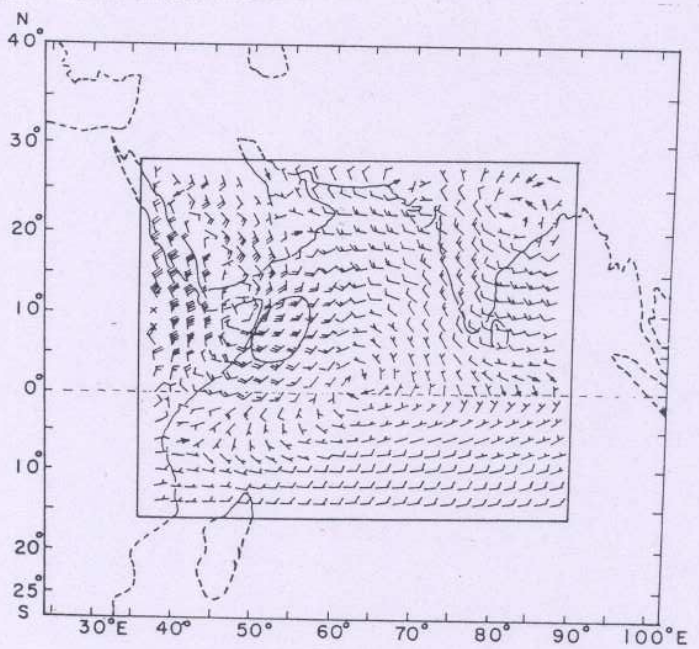

FIG. 9 : FORECAST WINDS AT 800 MB LEVEL

AO-EXPT, F.C. : 48-HOURS

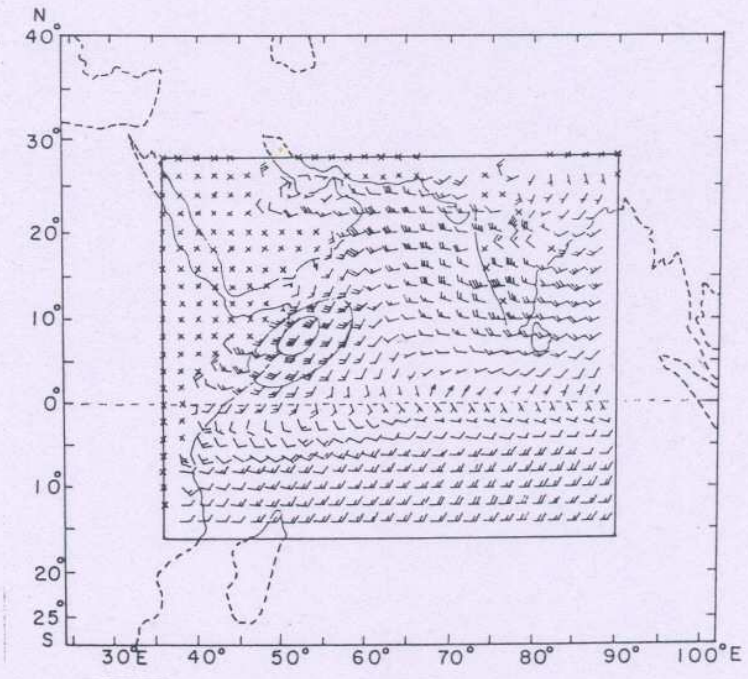

FIG. 10 : FORECAST WINDS AT 950 MB LEVEL

AO-EXPT., F.C. : 48-HOURS

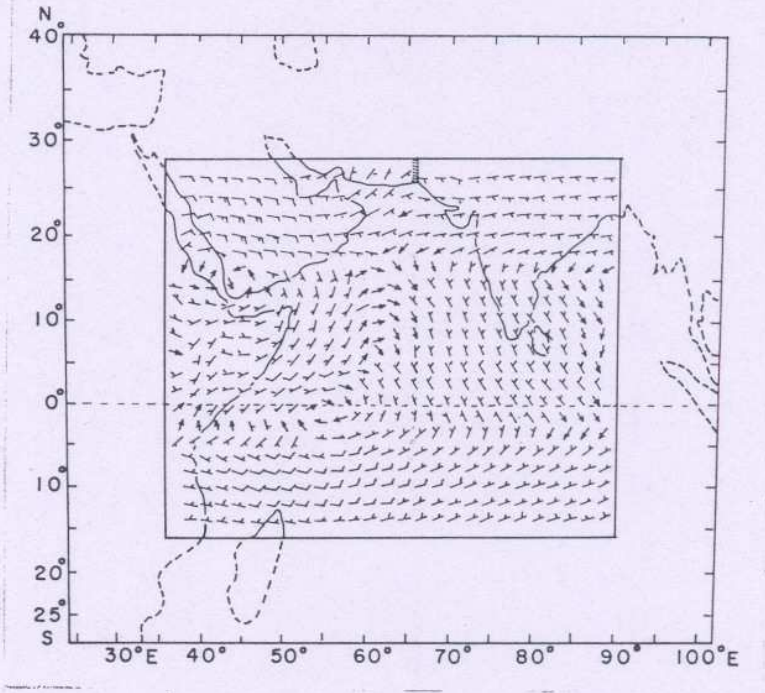

FIG. 11 : FORECAST WINDS AT 600 MB LEVEL

WI-EXPT., F.C. : 48-HOURS

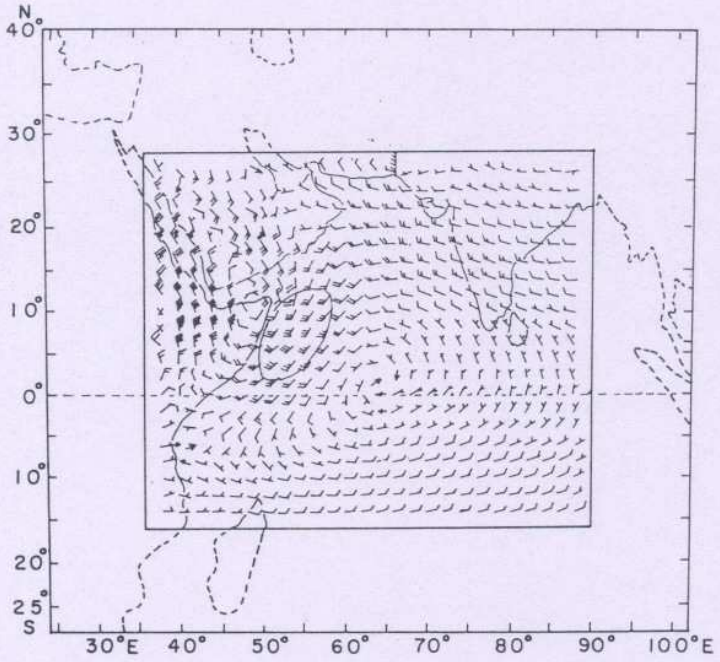

FIG.12: FORECAST WINDS AT 800-MB LEVEL

WI-EXPT., F.C. : 48-HOURS

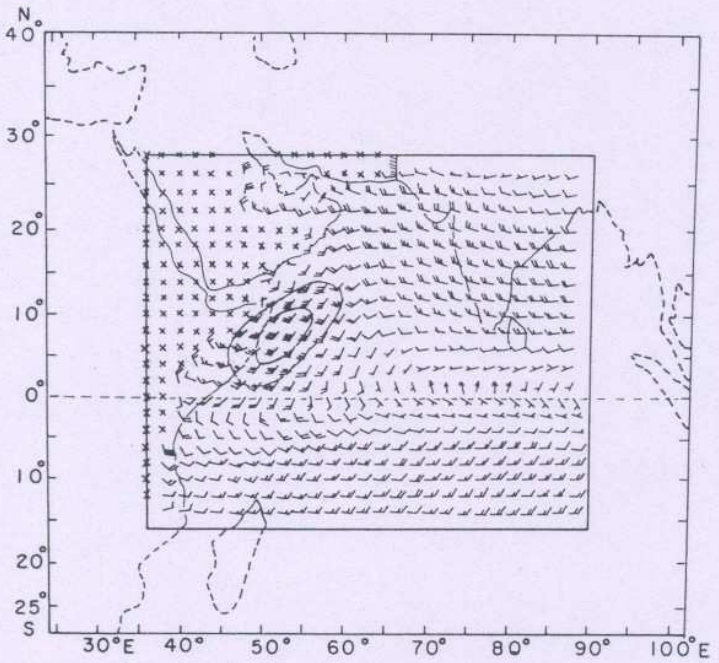

FIG.13: FORECAST WINDS AT 950 MB LEVEL

WI-EXPT., F.C.: 48-HOURS

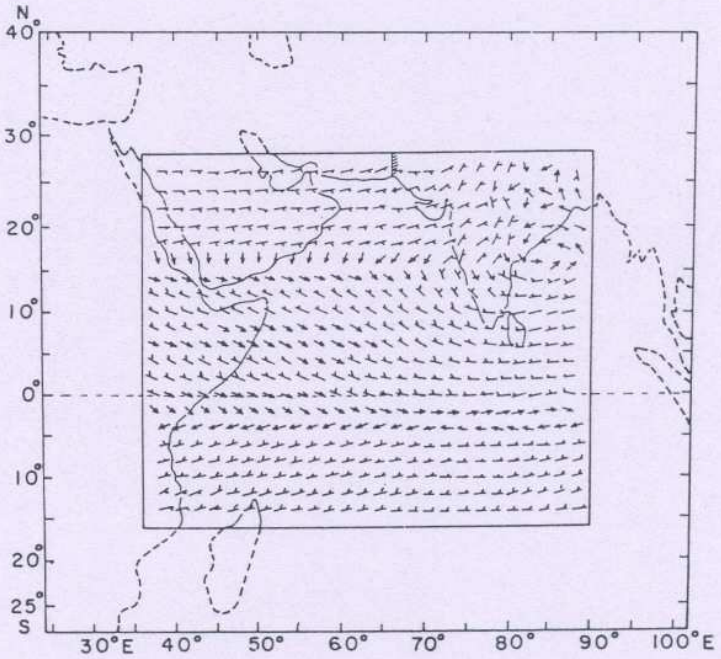

FIG.14: FORECAST WINDS AT 600 MB LEVEL

WA-EXPT., F.C. : 48-HOURS.

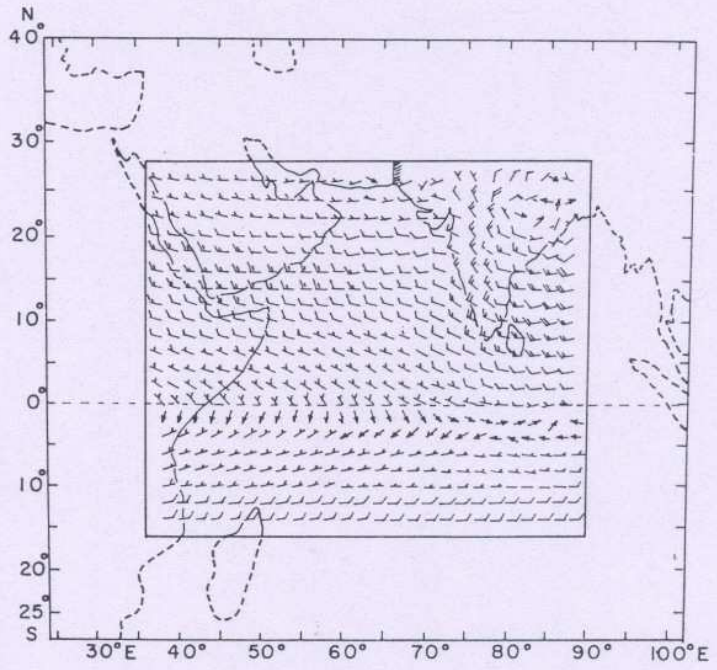

FIG.15: FORECAST WINDS AT 800 MB LEVEL

WA-EXPT., F.C.: 48-HOURS

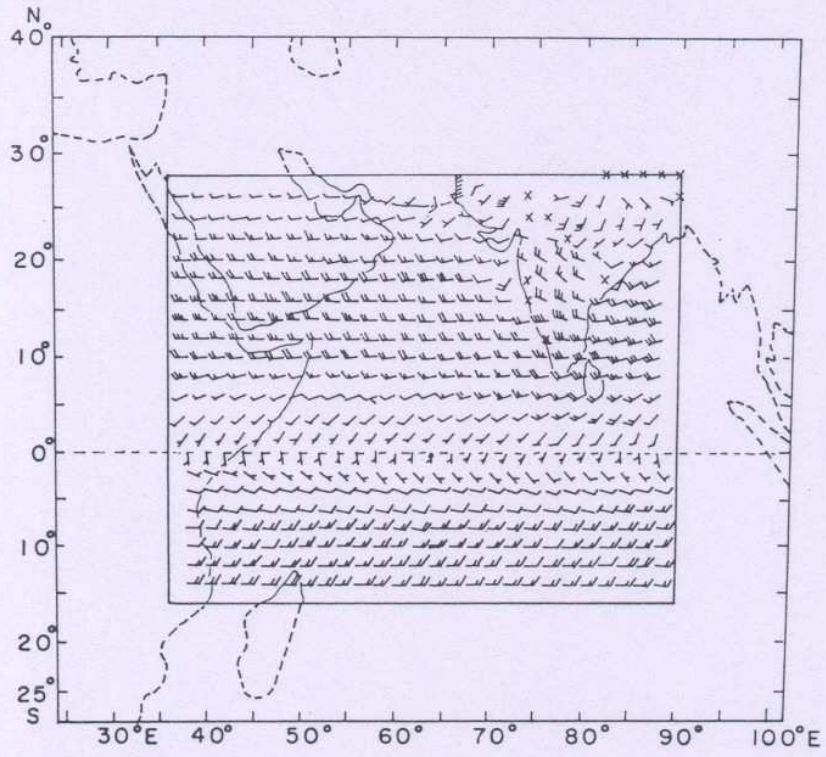

FIG.16 : FORECAST WINDS AT 950 MB LEVEL

WA-EXPT., F.C. : 48-HOURS.

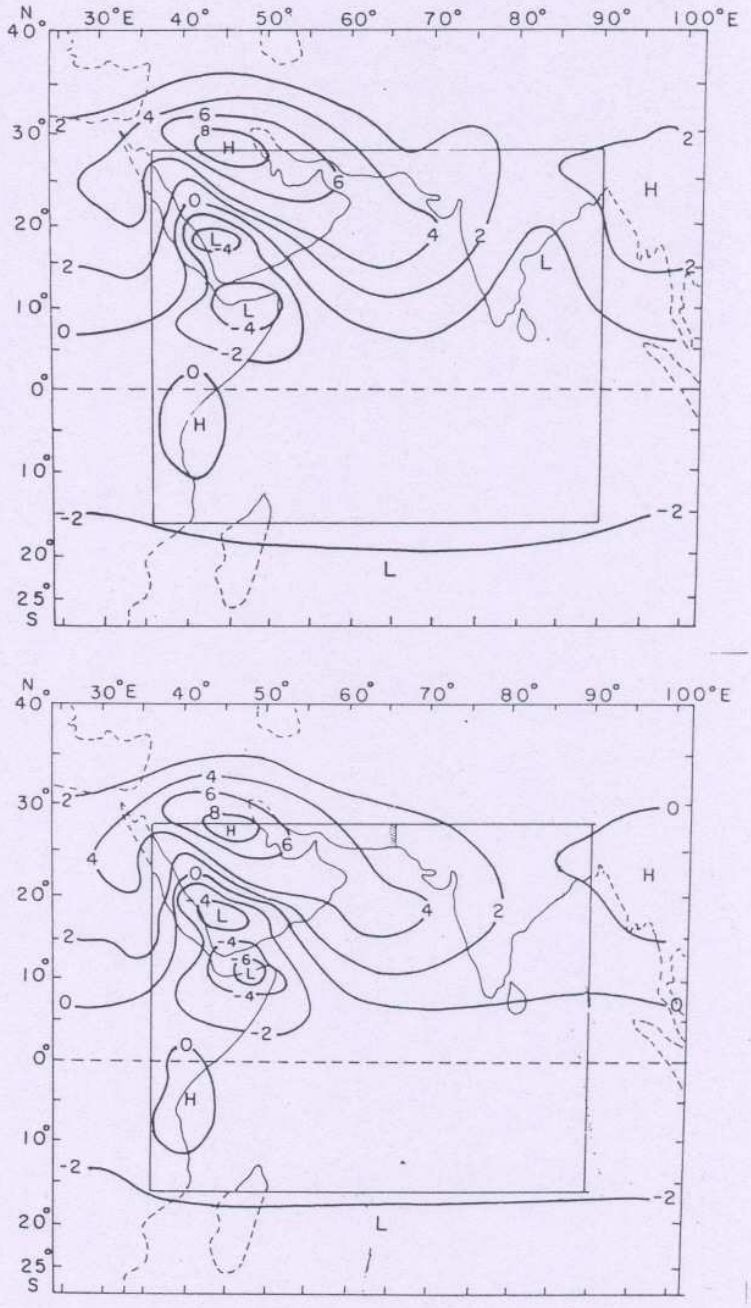

FIG. 17: SURFACE PRESSURE CHANGE FOR AO - AND WI-EXPERIMENTS. F.C. : 48-HOURS.

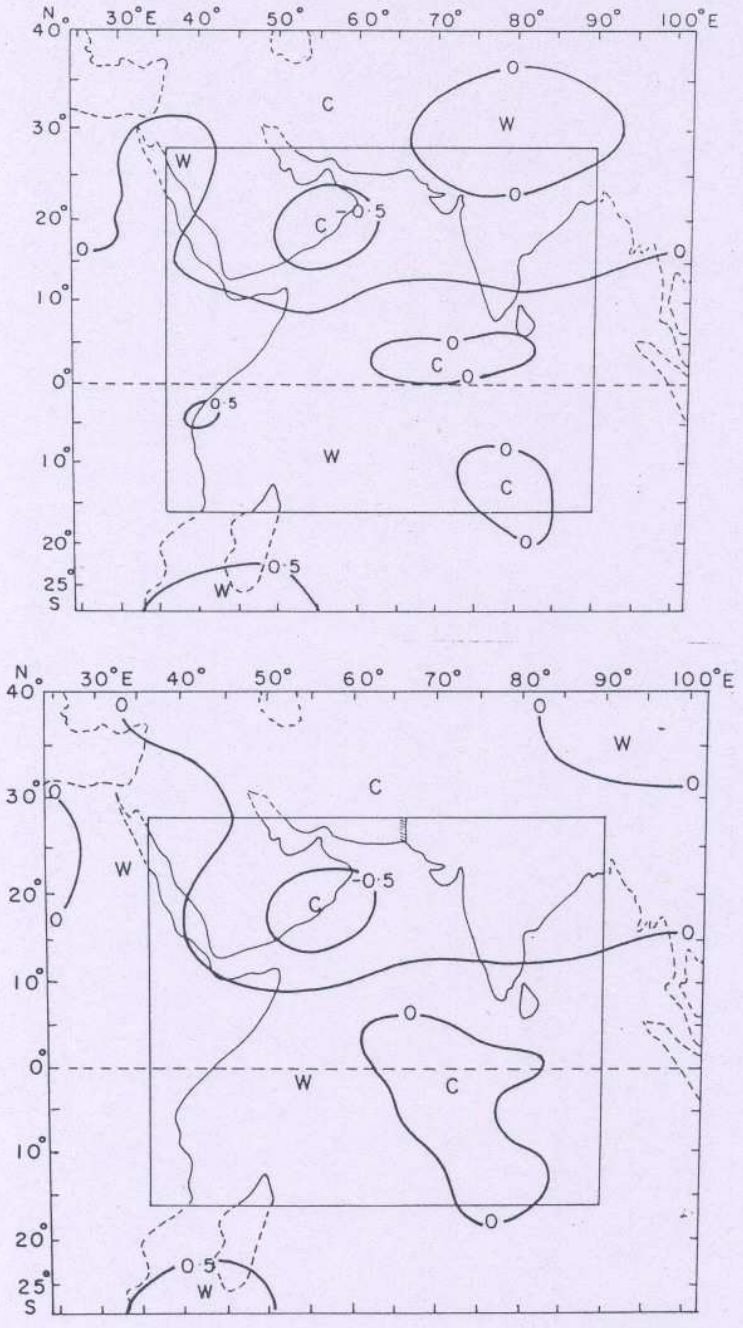

FIG.18: TEMPERATURE CHANGE AT 300 MB LEVEL

FOR AO-AND WI-EXPERIMENTS, F.C. : 48-HOURS

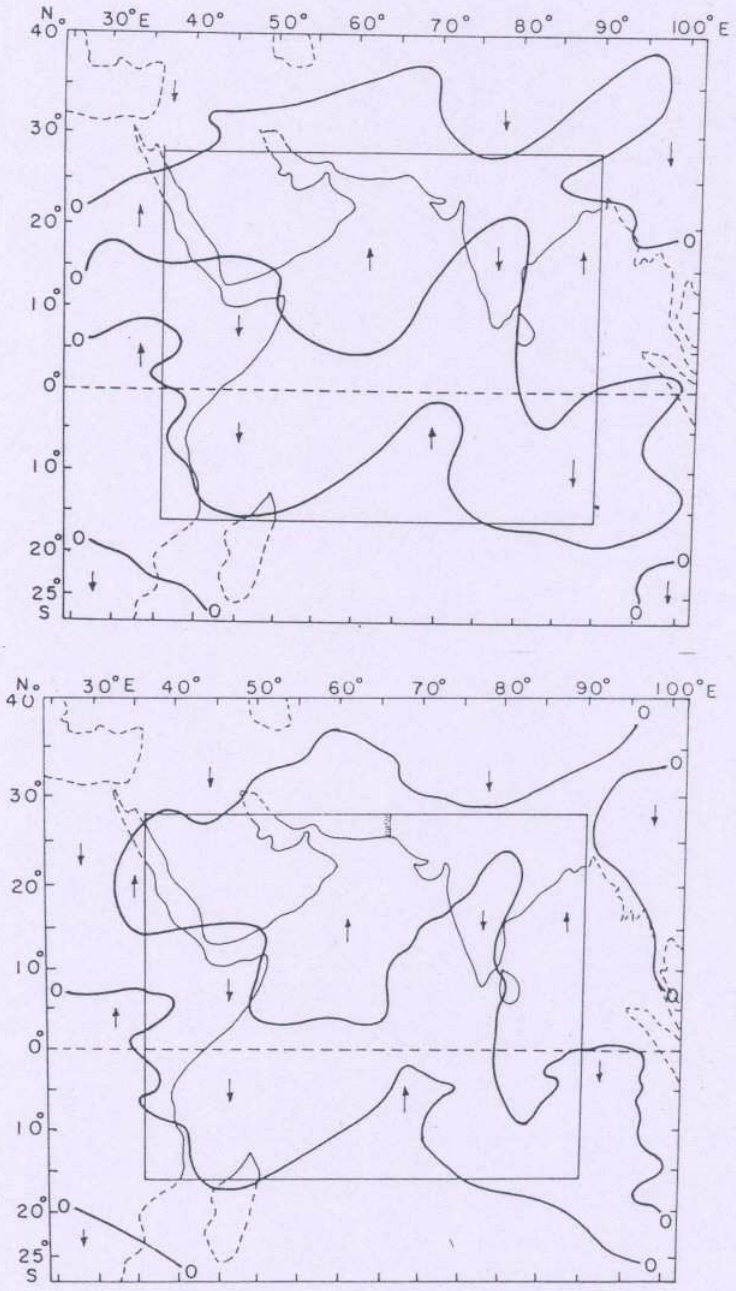

FIG. 19: VERTICAL P-VELOCITY AT 300-MB LEVEL
FOR AO-AND WI-EXPERIMENTS
F.C.: 48-HOURS, UNIT : 10^{-3} MB/SEC.

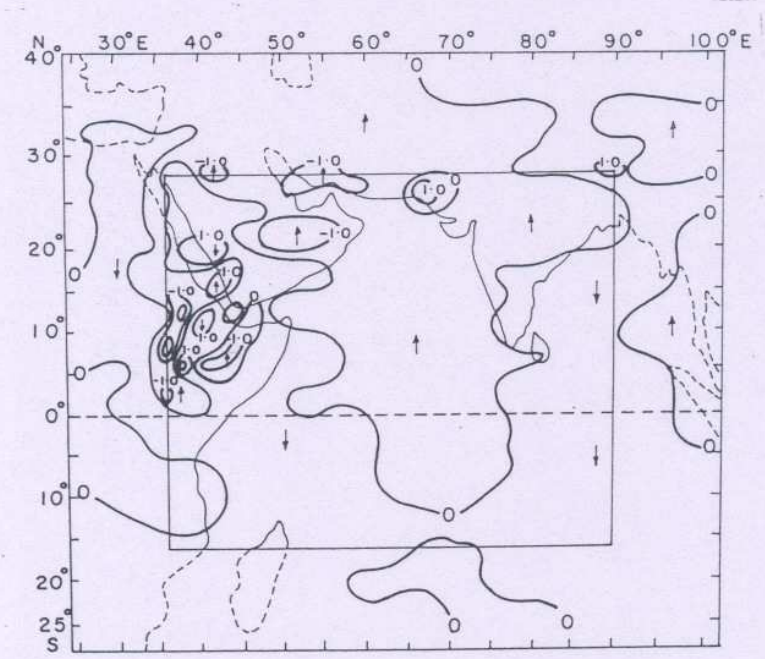

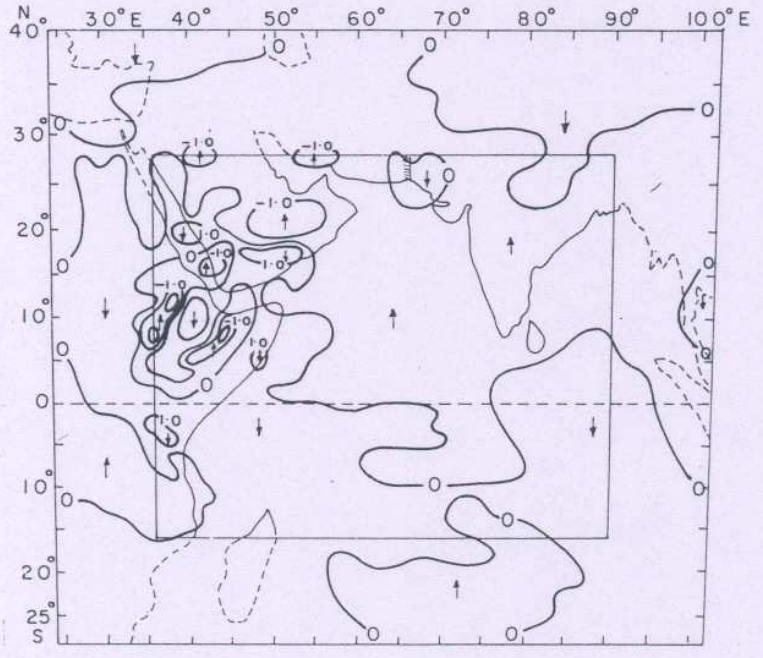

FIG.2o: VERTICAL P-VELOCITY AT 700 MB LEVEL FOR AO-AND WI-EXPERIMENTS.
F.C. : 48-HOURS. UNIT : 10^{-3} MB/SEC.

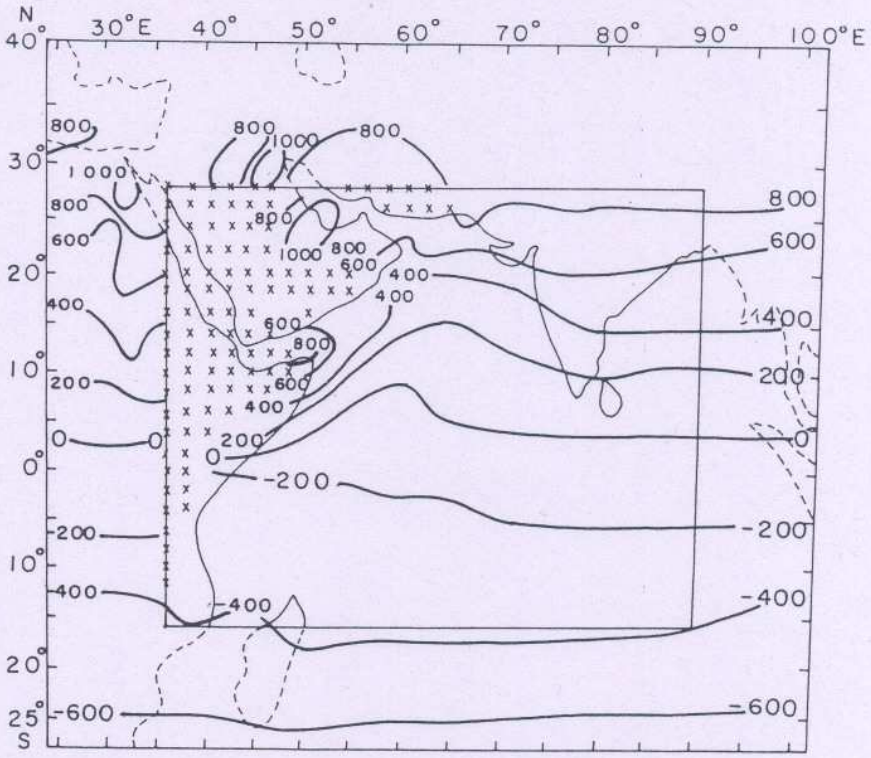

FIG. 21: ABSOLUTE VORTICITY η AT 950 MB LEVEL

FOR WI-EXPT., F.C. : 48-HOURS, UNIT : 10^{-7} SEC^{-1}

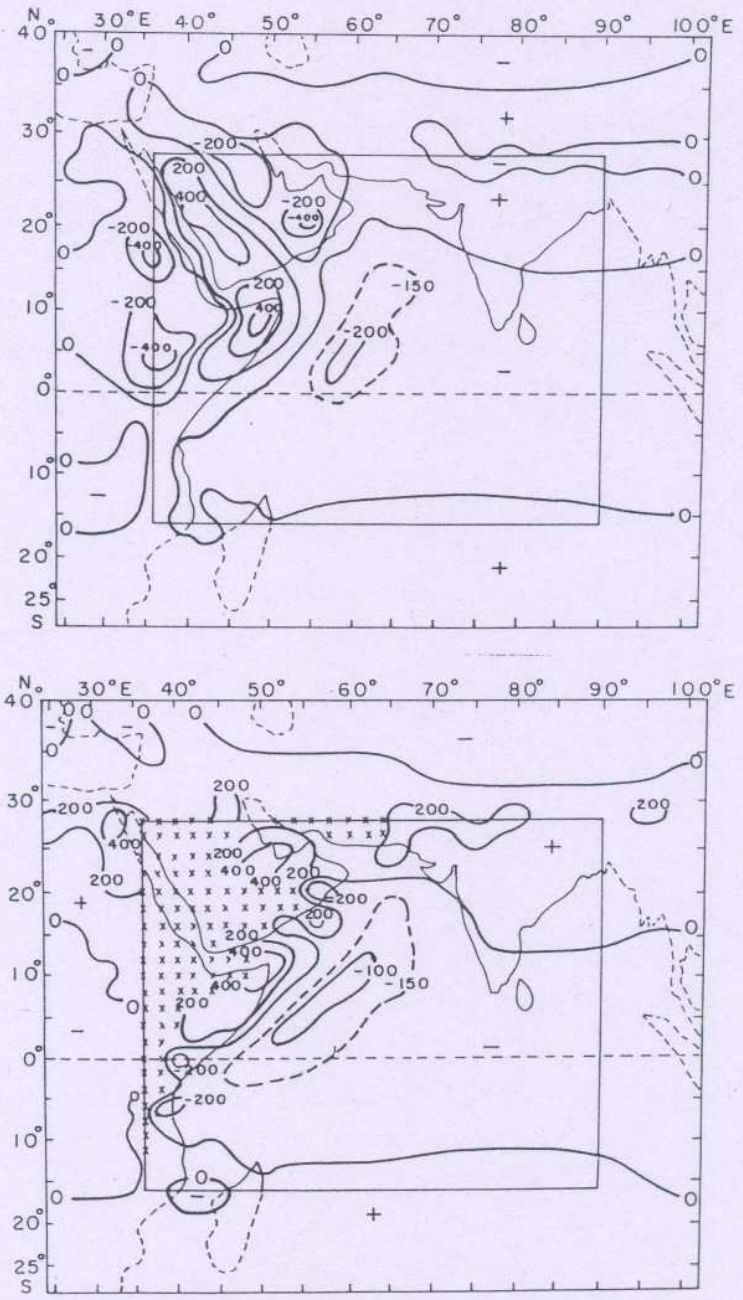

FIG. 22: RELATIVE VORTICITY ζ AT 800 and 950 MB LEVELS, FOR WI-EXPT., F.C. : 48-HOURS, UNIT : 10^{-7}SEC^{-1}.

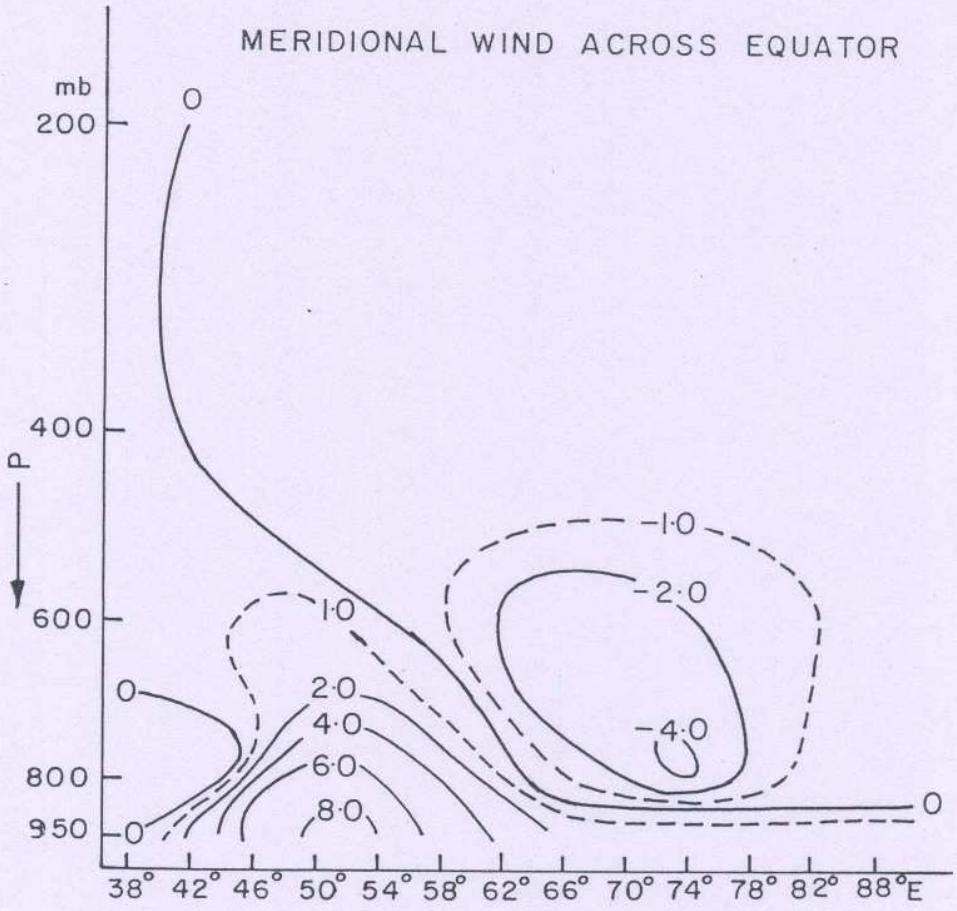

FIG.23: MERIDIONAL WIND ACROSS EQUATOR FOR AO-EXPERIMENT, F.C. 48-HOURS